Available online at www.sciencedirect.com

ScienceDirect

Nuclear Physics A 945 (2016) 134–143

NUCLEAR PHYSICS A

www.elsevier.com/locate/nuclphysa

Tentative study of nuclear charge radii for neutron-deficient nuclei around the $Z = 82$ shell from experimental α decay data

Yibin Qian [a,b,*], Zhongzhou Ren [b,c,d]

[a] *Department of Applied Physics, Nanjing University of Science and Technology, Nanjing 210094, China*
[b] *Department of Physics and Key Laboratory of Modern Acoustics, Nanjing University, Nanjing 210093, China*
[c] *Center of Theoretical Nuclear Physics, National Laboratory of Heavy-Ion Accelerator, Lanzhou 730000, China*
[d] *Kavli Institute for Theoretical Physics China, Beijing 100190, China*

Received 31 August 2015; received in revised form 9 October 2015; accepted 13 October 2015

Available online 23 October 2015

Abstract

We tentatively investigate the root-mean-square (rms) nuclear charge radii of odd-A Po and Pb isotopes plus Tl isotopes, particularly concerning these difficultly-detected nuclei along with short lifetimes, via various data on α decay. Within the density-dependent cluster model, the density distributions of studied daughter nuclei are determined by exactly reproducing the corresponding experimental α decay half-lives, which leads the final results of nuclear charge radii. In addition, our recently proposed formula deducing the charge radii is extended to this study for comparison. Whether it concerns the ground or isomeric state of target nuclei, the extracted nuclear charge radii are found to be in good agreement with the measured values. Sequential predictions on the rms charge radii are subsequently made for these neutron-deficient nuclei and especially for the rarely detected Bi isotopic chain, which are expected to be useful for future measurements. Moreover, the variety of α-preformation factors is analyzed in the scheme of valence nucleon number to pursue the further improvement of the model. This may be considered as an effective effort to obtain the charge radii of ground and even low-lying excited states for exotic nuclei near the proton-dripline.

* Corresponding author at: Department of Applied Physics, Nanjing University of Science and Technology, Nanjing 210094, China.
E-mail address: qyibin@njust.edu.cn (Y. Qian).

http://dx.doi.org/10.1016/j.nuclphysa.2015.10.002
0375-9474/

Keywords: α Decay; Cluster model; Nuclear charge radius

1. Introduction

Since the α particle scattering experiment proposed by Rutherford, the scattering cross section of α particles and even the α-decay half-lives have been employed to detect the size of an atomic nucleus (i.e., the nuclear radius) and its matter density distribution [1]. As one of the most fundamental bulk properties of a nucleus, the nuclear charge radius plays a key role in probing the nuclear shell structure and the effective interactions of nuclei such as the direct information on Coulomb energy of nuclei [2,3]. Impressively, the correlated phenomena such as shape coexistence, nuclear skin and halo are very attractive in contemporary nuclear physics as well as studying in nuclear astrophysics. Up to now, there have been several experimental sources providing the information on rms nuclear charge radii, including the electron or other particles (p, $\pi^{\pm}$, and μ) scattering on target nuclei, the measurements of transition energies of muonic atoms, the K_α X-ray and optical isotope shifts [2,3]. The measurements with electron scattering, μ^- atoms, and K_α X-ray can only be served for stable isotopes due to the experimental requirements for the quantities of target nuclei. Nevertheless, the optical isotope shifts (OIS) can be performed within even few radioactive atoms (ions) along with short lifetime down to 1 ms, indicating that it can be accessible to long chains of radioactive isotopes far away from the stability line. In the recent experimental studies of attractive shape coexistence across the $Z = 82$ proton shell closure and around the $N = 104$ midshell, isotope shifts have been measured for the neutron-deficient isotopes, leading to the new or improved data on changes in the mean square nuclear charge radii $\delta < r^2 >$ [4–7]. Meanwhile, quite a number of α decay data have been accumulated in this exotic region within improved accuracy [8–13].

Following the pioneer work about the quantum explanation of α decay as the tunneling effect, extensive theoretical approaches have been proposed to describe this radioactive process [14–31]. As phenomenological methods, analytical expressions such as the Viola–Seaborg formula [14] and some new laws for α decay and cluster radioactivity including more quantum ingredients [15–17], are employed to obtain the half-lives. Based on various effective α-nucleus potentials, considerable models have been conducted to pursue quantitative curve of α decay such as the generalized liquid droplet model [18], the united model for α decay and α capture [19–21], the density-dependent cluster model [24–28], and the Coulomb and Proximity potentials model for deformed nuclei [29], etc. In the recent studies of our group, the quantum solution of the Schrödinger equation within the double-folding potentials was performed to systematically calculate the α decay half-lives within a factor of 2 [30,31]. Inspired by the good agreement between theory and experiment in our work and the special role of α decay in the detection of nuclear charge radii, we proposed to deduce the nuclear charge radii with the help of the α decay cluster model [32,33]. Subsequently, nuclear charge radii of heavy and superheavy nuclei, including even–even, odd-A and odd–odd nuclei, have been successfully extracted from the experimental α decay data. In this effective way, the α decay spectroscopy is actually connected with the rms charge radii of nuclei. It is physically important to perform the study on more exotic nuclei, i.e., the neutron-deficient nuclei around the proton-dripline, especially concerning those target nuclei with half-lives below the experimental limitation. Impressively, we would pay more attention to the isomeric states of these exotic nuclei, which seems to be barely obtained in other theoretical studies focusing the ground-state properties for a number of nuclei such as the evaluations of charge radii based on the mass model [34,35]. This study can further check the validity of

the present approach and provide more valuable information about nuclear charge radii directly related with nuclear shapes.

In the following of this article, Section 2 presents a brief introduction of the present framework for deducing the nuclear charge radii. Numerical results and corresponding discussions are shown in Section 3, and a summary is given in the last section.

2. Theoretical framework

Owing to the significant developments of available experimental methods such as the electron or muon scattering, nuclear charge distribution and radii have been accurately obtained for many nuclei [2,3,36]. Unfortunately, our experimental knowledge about the neutron distribution of one nucleus and its radius is still quite insufficient [37,38]. Although the neutron radius or the neutron skin of the typical nucleus ^{208}Pb has been detected in the very recent experiments [39,40], the corresponding experimental value appears to be uncertain and the information on neutron radii of a large range of nuclei is extremely limited. Considering the few recognition of neutron distribution in nuclei, we preliminarily take the same form to depict the proton and neutron distributions [32,33]. In the parent nucleus involved in the α decay process, usually regarded as a two-body system of an α particle interacting with an axially symmetric deformed core nucleus, the nucleon and charge density distributions of the daughter nucleus are both assumed to behave in the two-parameter Fermi form

$$\rho_1(r_1,\theta_1) = \frac{\rho_0}{1+\exp\left[\frac{r_1-R_{1/2}(\theta_1)}{a}\right]}. \tag{1}$$

Here θ_1 is the angle between $\vec{r_1}$ (related to the nucleon) and the symmetric axis of the daughter nucleus. The half-density radius $R_{1/2}(\theta_1)$ is parameterized as

$$R_{1/2}(\theta_1) = r_0 A_d^{1/3}[1+\beta_2 Y_{20}(\theta_1)+\beta_4 Y_{40}(\theta_1)]. \tag{2}$$

The ρ_0 value is determined by integrating the density distribution equivalent to the mass or atomic number of the target daughter nucleus, and β_2 and β_4 are its quadrupole and hexadecapole deformation parameters [35]. After taking the widely-used Gaussian density distributions ρ_2 of the spherical α particle, the nuclear and Coulomb interaction potentials can be obtained from the double folding integral

$$V_{N\,\mathrm{or}\,C}(r,\theta) = \iint d\mathbf{r_1}\, d\mathbf{r_2}\ \rho_1(\mathbf{r_1})\upsilon(\mathbf{s}=|\mathbf{r_2}+\mathbf{r}-\mathbf{r_1}|)\rho_2(\mathbf{r_2}), \tag{3}$$

where θ is the orientation angle of the emitted α particle with respect to the symmetric axis of the core nucleus, and $\upsilon(\mathbf{s})$ represents the realistic M3Y-Reid-type nucleon–nucleon (NN) interaction and the standard Coulomb force for the nuclear potential and the Coulomb one, respectively. Consequently, the total interaction potential of α-core system consisting of the nuclear and Coulomb terms is given by

$$V(r,\theta) = \lambda V_N(r,\theta) + V_C(r,\theta), \tag{4}$$

where λ is the renormalization factor for nuclear potential. For one certain orientation angle θ, the total potential $V(r,\theta)$ is subsequently reduced into a one-dimensional case, i.e., $V(r)$. The potential $V(r)$ is then divided into two components: the "inner" part and the "outer" term by a separation radius R_0 within the modified two-potential approach. The radial Schrödinger equation with the inner potential is numerically solved to get the bound state wave function $\phi_{n\ell j}(r)$,

sharply vanishing in an exponential way from the separation radius R_0 [31]. During this procedure, the λ factor is determined by adjusting the experimental Q value and the special number n of internal nodes restricted by the Wildermuth condition containing the main effect of the Pauli principle [41]. One can then obtain the decay width for one certain angle,

$$\Gamma(\theta) = \frac{\hbar^2 k}{\mu}\left[\frac{\phi_{n\ell j}(\bar{r})}{G_\ell(k\bar{r})}\right]^2, \tag{5}$$

where the wave number k is $\sqrt{2\mu Q}/\hbar$, and G_ℓ is the irregular Coulomb wave function. The value of $\bar{r}$ is chosen in such a way that the potential $V(r)$ can be well approximated by the repulsive part (the attractive part disregards) for $r \geq \bar{r}$, and the above result is independent of R_0 or $\bar{r}$. Through an overall averaging process of $\Gamma(\theta)$, the final decay width is ultimately given by

$$\Gamma = \int_0^{\pi/2} \Gamma(\theta)\sin(\theta)d\theta, \tag{6}$$

reaching the α decay half-life $T_{1/2} = \hbar \ln 2/P_\alpha \Gamma$. Here the indispensable quantity P_α denotes the preformation probability of an α particle in the parent nucleus. In view of the available experimental analysis [42] and other α decay studies [25,30], the α-preformation factor is taken as the same constant for one kind of nuclei, to keep the numbers of free parameters to a minimum as well. Previously, the radius parameter r_0 and the diffuseness parameter a in the $\rho_1(r_1, \theta_1)$ are chosen as $r_0 = 1.07$ fm and $a = 0.54$ fm according to the nuclear textbook [1,43] subsequently resulting in the final decay half-lives. In turn, these mentioned parameters are fixed by exactly reproducing the experimental α decay half-lives to achieve the nuclear charge radii via the relationship

$$R \equiv \sqrt{< r^2 >} = \left[\frac{\iint \rho_1(r, \theta_1) r^4 \sin\theta_1 dr d\theta_1}{\iint \rho_1(r, \theta_1) r^2 \sin\theta_1 dr d\theta_1}\right]^{1/2}. \tag{7}$$

Keeping in mind the more sensitivity of half-lives to the r_0 factor as compared to the a value, the quantity r_0 is considered as the representation of the density distribution and the a value is taken as the suggested constants. Provided the discrepancies of the diffuseness parameter a for nuclei in the different mass regions, it is chosen as $a = 0.54$ fm for heavy nuclei with $N > 126$, and $a = 0.52$ fm for medium nuclei with $N \leq 126$ [44]. It is to be noted that the r_0 values for nucleon (proton and neutron) and charge density distribution are correlated by the existing expression $< r^2 >_c = < r^2 >_p + 0.64$ fm^2, along with the identical diffuseness parameter. Consequently, r_0 connects the rms nuclear charge radii and the corresponding α decay half-lives. Accounting these, the measured α decay half-lives are found to be well reproduced with the following case: $P_\alpha^{odd\text{-}A} = 0.094$ for odd-A nuclei and $P_\alpha^{odd\text{–}odd} = 0.084$ for odd–odd nuclei, based on the available experimental values of charge radii for the present studied nuclei. Obviously, these two values are both smaller than that of even–even nuclei obtained in our previous studies [32] besides the discrepancy between themselves, which is presumptive due to the unpaired nucleons and the proton–neutron correlations. Strikingly, the behavior of the preformation factor will be discussed to some extent in the next section.

3. Detailed results and discussions

By means of the highly sensitive in-source laser photoionization spectroscopy technique, nuclear charge radii have been directly probed into for the neutron-deficient nuclei such as isotopes

Table 1
Comparison of extracted rms nuclear charge radii with available experimental values for neutron-deficient isotopes near $Z = 82$, including the evaluation given by the expression (8). The symbols 'm' denotes the isomeric states.

Nuclei	I^π	R_{expt} (fm)	R_{calc1} (fm)	R_{calc2} (fm)	R_{calc3} (fm)	R_{form} (fm)
^{193}Po	$3/2^-$	5.52	5.43	5.43	5.43	5.55
^{193}Po^{m}	$13/2^+$	5.52	5.52	5.53	5.53	5.63
^{195}Po	$3/2^-$	5.52	5.61	5.62	5.62	5.55
^{195}Po^{m}	$13/2^+$	5.52	5.63	5.63	5.63	5.57
^{197}Po	$3/2^-$	5.51	5.45	5.45	5.45	5.45
^{197}Po^{m}	$13/2^+$	5.51	5.40	5.40	5.40	5.40
^{199}Po	$3/2^-$	5.51	5.50	5.50	5.50	5.55
^{199}Po^{m}	$13/2^+$	5.52	5.53	5.53	5.53	5.57
^{203}Po	$5/2^-$	5.53	5.50	5.50	5.50	5.57
^{187}Pb	$3/2^-$	5.41	5.20	5.20	5.20	5.22
^{187}Pb^{m}	$13/2^+$	5.41	5.48	5.49	5.48	5.48
^{189}Pb	$3/2^-$	5.42	5.28	5.28	5.28	5.31
^{189}Pb^{m}	$13/2^+$	5.42	5.31	5.31	5.31	5.32
^{183}Tl	$1/2^+$	5.38	5.33	5.33	5.33	5.31
^{185}Tl	$1/2^+$	5.39	5.31	5.31	5.31	5.33
^{185}Tl^{m}	$9/2^-$	5.41	5.46	5.46	5.46	5.39
^{186}Tl^{m}	10^-	5.41	5.41	5.41	5.41	5.35
^{187}Tl^{m}	$9/2^-$	5.42	5.48	5.48	5.48	5.43
^{189}Tl^{m}	$9/2^-$	5.43	5.42	5.42	5.42	5.41
^{191}Tl	$1/2^+$	5.42	5.40	5.40	5.40	5.38
^{191}Tl^{m}	$9/2^-$	5.43	5.36	5.36	5.36	5.39

with $Z = 81, 82,$ and 84 across the $Z = 82$ proton shell and around the $N = 104$ midshell [5–7]. As well, α decay studies have already been devoted to detect the features of these exotic nuclei in the ground or low-lying isomeric states [6,10–13]. To this end, we have initially paid attention to the available experimental values of charge radii in Tl, Pb, and Po isotopes, especially for odd-A and odd–odd nuclei providing valuable information on exotic structural phenomenon, via α decays to these nuclei. In detail, no matter what it concerns ground or isomeric states for the target nuclei, the spin–parity of parent nuclei is chosen as the identical one of daughter nuclei resulting in the favored α transitions ($\ell = 0$). Besides the introduced theoretical approach, a simple relation between the rms nuclear charge radii and the α decay data, namely

$$\sqrt{R} = (c_1 - c_2 \log_{10} T_{1/2})/\xi_1\xi_2 + c_3\xi_1 Q_\alpha^{-1/2} \tag{8}$$

was proposed by our group, which is also used to evaluate the charge radii for comparison. Here $\xi_1 = \sqrt{Z_c Z_d e^2}$, $\xi_2 = \sqrt{2\mu}/\hbar$, and the three parameters c_1, c_2, c_3 are determined by fitting the available experimental data. For the case of odd–odd nuclei, the measured data appear to be not enough in the fitting process. However, it is found that the results from Eq. (8) with these fitted parameters for odd-A nuclei are consistent with the few experimental radii and corresponding calculated ones of odd–odd nuclei. With this in mind, we apply the formula (8) with an identical set of parameters directly taken from our previous study [33], to evaluate the charge radii of both odd-A and odd–odd nuclei. Additionally, the experimental α decay energies and half-lives, from the AME2012 table [8,9] and the NNDC database [45], are employed to obtain the charge radii of target isotopes.

As mentioned before, various studies within the folding model [24–28] have been devoted to evaluating the α-core potential along with various NN interactions and slightly different forms

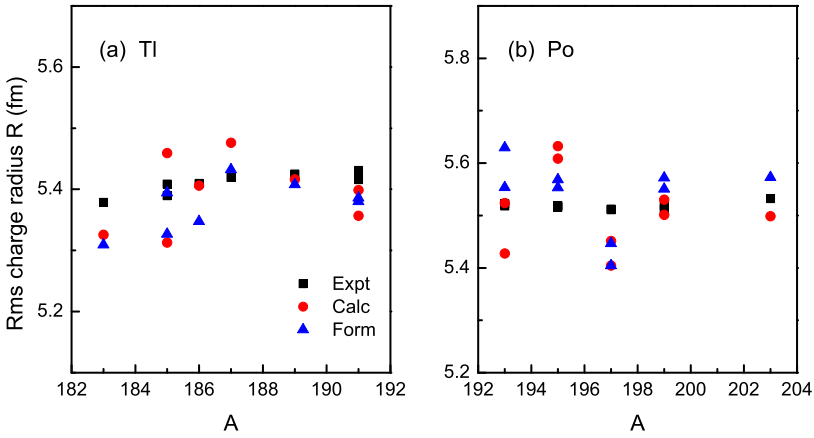

Fig. 1. Comparison of the extracted rms nuclear charge radii with the experimental data for (a) Tl and (b) Po isotopes including both the ground and isomeric states.

Table 2
Predicted charge radii for the ground and isomeric states of neutron-deficient isotopes of elements Pb and Tl, based on the available experimental data of α decay.

Nuclei	I^π	R_{calc} (fm)	R_{form} (fm)
^{191}Pb^m	$13/2^+$	5.39	5.41
^{193}Pb^m	$13/2^+$	5.43	5.47
^{195}Pb^m	$13/2^+$	5.48	5.53
^{197}Pb^m	$13/2^+$	5.39	5.47
^{199}Pb^m	$5/2^-$	5.39	5.50
^{182}Tl^m	10^-	5.31	5.31
^{183}Tl^m	$9/2^-$	5.44	5.45
^{184}Tl^m	3^+	5.38	5.38
^{184}Tl^n	10^-	5.36	5.38
^{186}Tl^m	3^+	5.39	5.43
^{187}Tl	$1/2^+$	5.34	5.38
^{188}Tl^m	3^+	5.48	5.44
^{188}Tl^n	10^-	5.42	5.38
^{189}Tl	$1/2^+$	5.43	5.48
^{190}Tl^m	3^+	5.52	5.50
^{190}Tl^n	10^-	5.40	5.40

of the density distribution of daughter nuclei. To perform the comparative study, we also employ another two folding integral α-daughter potentials in the present calculation: one using the same M3Y-Reid NN interaction but with a different form of the half-density radius in the density distribution from Ref. [24]

$$R_{1/2}(\theta_1) = r_0 A_d^{1/3}[1 - \pi^2 a^2/3r_0^2 A_d^{2/3}][1 + \beta_2 Y_{20}(\theta_1) + \beta_4 Y_{40}(\theta_1)], \tag{9}$$

and the other with the same form of the density distribution but using the M3Y-Paris NN interaction [26]. Table 1 represents the detailed results for Po, Pb, and Tl isotopes, and the first two columns list the target nuclei along with their spin–parity. The following columns respectively denote the measured charge radii [5–7] and the calculated values in the present approach and

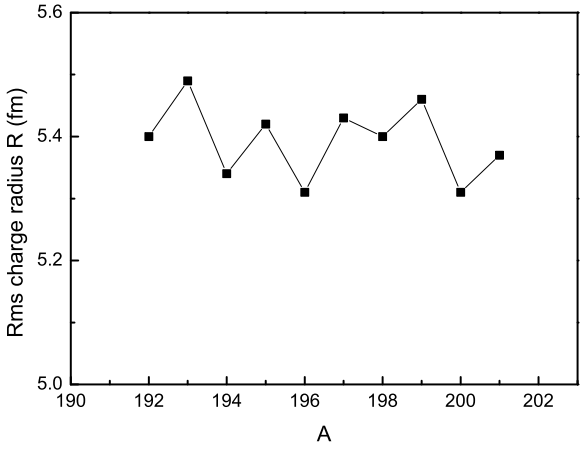

Fig. 2. Deduced nuclear charge radii of the Bi isotope ground states versus the mass number.

Eq. (8). The calculated results in the framework of the previous section and the above two cases are denoted as 'calc 1', 'calc 2', and 'calc 3' in sequence. One can see that these three groups of results are very close to each other, implying the tiny influence of the specific form of the density distribution and the NN interaction (in the folding model) on the final extracted radius for daughter nuclei to some extent. Hence we just take the first case 'calc 1' described in the theoretical framework of Section 2 in the following illustration and calculation of this study, for the sake of convenience. By comparing with the available experimental charge radii, the standard deviation of our calculated results is obtained as $\sigma = \left[\sum_{i=1}^{21}(R^i_{\rm expt} - R^i_{\rm calc})^2/21\right]^{1/2} = 0.08$ fm, indicating a good agreement between theory and experiment. For a better insight, we plot the experimental rms charge radii and the deduced ones versus the mass number of studied nuclei in Fig. 1. Note that the previously studied Pb isotopes in the ground states [32,33] are not included in this work, and Fig. 1 focuses the ground and isomeric states of Tl and Po isotopes. As can be seen, the extracted charge radii generally lie around the experimental values, and are consistent with those estimated ones by the relation of charge radii with the decay data. Encouraged by this, we subsequently extend the study to the unknown charge radii of these isotopes, and the detailed predictions are shown in Table 2. The last two columns list our results and the estimated ones by Eq. (8), which are consistent with each other. For these proton-rich nuclei, the occupy behavior of the valence protons, extensively related with charge radii, could be different from the standard case of the spherical shell model due to the weak binding energies and the deformations. This could lead to the smooth change or slight fluctuation of the nuclear charge radii for these neutron-deficient isotopes in the vicinity of the proton-dripline, as shown in Tables 1, 2 and Fig. 1.

Besides, it is of great interest to probe into the Bi isotopic chain, considering that these neutron-deficient nuclei are very close to the $Z = 82$ proton shell while the experimental detection appears to be relatively rare. On the basis of the available experimental data of α decay, we systematically investigate the charge radii of Bi isotopes, as listed in Table 3. In order to pursue the recognition of the possible structural evolution in this isotopic chain, the nuclear charge radii of the Bi isotope ground states are plotted versus the mass number in Fig. 2, including both odd-A and odd–odd nuclei. Interestingly, in contrast to the Tl isotopic chain where unobvious odd–even staggering is presented [7], there seems to be odd–even staggering for charge radii of

Table 3
Extracted nuclear charge radii for various Bi isotopes in the ground and isomeric states, to be somewhat helpful for future detection.

Nuclei	I^π	$R_{\rm calc}$ (fm)	$R_{\rm form}$ (fm)
^{187}Bi$^{\rm m}$	$7/2^-$	5.42	5.41
^{188}Bi$^{\rm m}$	$(9,10)^-$	5.31	5.32
^{189}Bi$^{\rm m}$	$1/2^+$	5.54	5.54
^{189}Bi$^{\rm n}$	$7/2^-$	5.45	5.46
^{189}Bi$^{\rm p}$	$13/2^+$	5.47	5.49
^{191}Bi$^{\rm m}$	$1/2^+$	5.51	5.54
^{191}Bi$^{\rm n}$	$7/2^-$	5.46	5.48
^{192}Bi	3^+	5.40	5.42
^{193}Bi	$9/2^-$	5.49	5.52
^{193}Bi$^{\rm m}$	$1/2^+$	5.45	5.50
^{194}Bi	3^+	5.34	5.39
^{194}Bi	10^-	5.44	5.47
^{195}Bi	$9/2^-$	5.42	5.48
^{196}Bi	3^+	5.31	5.38
^{196}Bi$^{\rm m}$	7^+	5.34	5.41
^{196}Bi$^{\rm n}$	10^-	5.34	5.41
^{197}Bi	$9/2^-$	5.43	5.51
^{198}Bi	$(2,3)^+$	5.40	5.47
^{198}Bi$^{\rm m}$	7^+	5.30	5.39
^{198}Bi$^{\rm n}$	10^-	5.41	5.48
^{199}Bi	$9/2^-$	5.46	5.55
^{200}Bi	7^+	5.31	5.41
^{201}Bi	$9/2^-$	5.37	5.48
^{202}Bi$^{\rm m}$	5^+	5.32	5.44

the ground states in Bi isotopes beyond the $N = 104$ midshell, which may be caused by the occupation of the $\pi h_{9/2}$ intruder orbital for the odd proton. This could be an exotic phenomena to be further detected for the experimentalists. As noted above, the feature that the charge radii of the Bi isotopes do not always increase with the mass number may be caused by the influence of the unpaired valence nucleons. In addition, the α preformation factor should be reduced when approaching the shell closure, and the used P_α value is then larger than its supposed one for nuclei close to the shell. Consequently, smaller r_0 and corresponding charge radii are produced, which may result in the decrease trend of charge radii for nuclei near the $N = 126$ neutron shell. It is of physical significance to account the structural factor such as the energy levels and pairing interaction [26], the valence nucleon number [28], etc., to improve the description of α-preformation factor.

In the following, we would like to initially analyze the varying trend of α-preformation factor in the N_pN_n scheme, where the effective number of valence nucleons $N_{p,n}$ is the difference between the nucleon number of parent nuclei and the nearest closed-shell number. In detail, we deduce the r_0 value of ρ_1 from the available experimental charge radius and calculate the α decay half-life $T^{\rm calc}_{1/2}$ without P_α. Then the preformation factor is extracted as the ratio of the calculated value to the experimental one, namely $T^{\rm calc}_{1/2}/T^{\rm expt}_{1/2}$, whose logarithm is plotted versus the product N_pN_n for odd-A nuclei in Fig. 3. It is seen that the $\log_{10} P_\alpha$ value generally varies slightly and smoothly while the slope of the linear-fitted line is almost zero. This somewhat prove the validity of the present treatment for constant P_α. However, this initial analysis is restricted to a

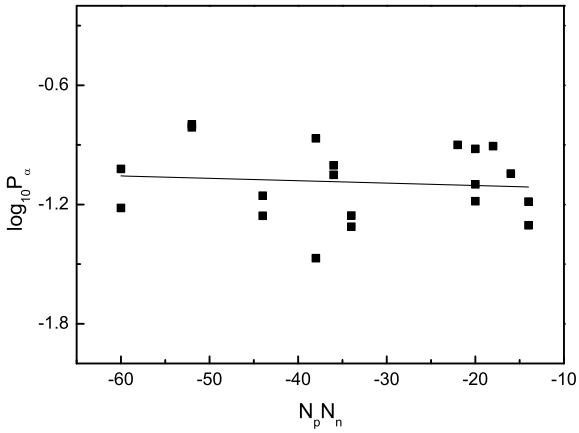

Fig. 3. Extracted preformation factors vary with N_pN_n values for odd-A nuclei in the Tl, Pb, and Po isotopes along with a linear-fitted line, where $N_p = Z - Z_0$ and $N_n = N - N_0$. For the present case, the nearest proton and neutron shell numbers Z_0 and N_0 are respectively taken as 82 and 126.

certain range of nuclei around $Z = 82$ and with the open-shell neutron number. The systematical behavior of α-preformation factor needs more attention in the pursuit of the higher accuracy for the calculation of rms charge radii, and this is worth further investigation. Besides, the expression (8) can be enhanced by adding a N_pN_n-related term in the first bracket by revisiting the deduction process. Afterwards, it should be very interesting to correlate the nuclear charge radii of neutron-deficient nuclei around the proton-dripline, with more new or improved experimental decay data in the future experiments.

4. Summary

To conclude, the density-dependent cluster model combined with the two-potential framework have been developed to pursue the rms nuclear charge radii of exotic nuclei in the neutron-deficient region from the experimental α decay data. As the source of the rms nuclear charge radii, the density distribution of focused daughter nuclei involved in the double-folding potential is adjusted by exactly matching the measured α decay half-lives. The extracted results of nuclear charge radii are shown in good agreement with the available experimental values for both the ground and isomeric states, and found to be consistent with the evaluations from our previously proposed formula. Moreover, unknown charge radii of these neutron-deficient nuclei near the proton-dripline are tentatively predicted. Especially, there seems to be interesting staggering of odd–even effects in the Bi isotope ground states, which may deserve further observation. The α-preformation factor is preliminarily discussed in the valence nucleons scheme to seek the promotion of the present model as well. It is hoped that the present study could be useful for future experiments on exotic nuclei with short lifetimes, whose charge radii are difficult to be measured.

Acknowledgements

This work is supported by the National Natural Science Foundation of China (Grants No. 11035001, No. 10975072, No. 10735010, No. 11375086, and No. 11120101005), by the 973 National Major State Basic Research and Development Program of China (Grant No.

2013CB834400), by a Project funded by the Priority Academic Programme Development of Jiangsu Higher Education Institutions (PAPD), and by the Natural Science Youth Fund of Jiangsu Province (Grant No. BK20150762).

References

[1] A. Bohr, B.R. Mottelson, Nuclear Structure, World Scientific, Singapore, 1998.
[2] I. Angeli, At. Data Nucl. Data Tables 87 (2004) 185.
[3] I. Angeli, K.P. Marinova, At. Data Nucl. Data Tables 99 (2013) 69.
[4] H. De Witte, et al., Phys. Rev. Lett. 98 (2007) 112502.
[5] M.D. Seliverstov, et al., Eur. Phys. J. A 41 (2009) 315.
[6] M.D. Seliverstov, et al., Phys. Lett. B 719 (2013) 362.
[7] A.E. Barzakh, et al., Phys. Rev. C 88 (2013) 024315.
[8] M. Wang, G. Audi, A.H. Wapstra, F.G. Kondev, M. MacCormick, X. Xu, B. Pfeiffer, Chin. Phys. C 36 (2012) 1603.
[9] G. Audi, F.G. Kondev, M. Wang, B. Pfeiffer, X. Sun, J. Blachot, M. MacCormick, Phys. Rev. C 36 (2012) 1157.
[10] A.N. Andreyev, et al., Phys. Rev. C 73 (2006) 044324.
[11] A.N. Andreyev, et al., Phys. Rev. C 80 (2009) 024302.
[12] A.N. Andreyev, et al., J. Phys. G, Nucl. Part. Phys. 37 (2010) 035102.
[13] A.N. Andreyev, et al., Phys. Rev. Lett. 110 (2013) 242502.
[14] V.E. Viola, G.T. Seaborg, J. Inorg. Nucl. Chem. 28 (1966) 741.
[15] Tiekuang Dong, Zhongzhou Ren, Eur. Phys. J. A 26 (2005) 69.
[16] Dongdong Ni, Zhongzhou Ren, Tiekuang Dong, Chang Xu, Phys. Rev. C 78 (2008) 044310.
[17] Yuejiao Ren, Zhongzhou Ren, Phys. Rev. C 85 (2012) 044608.
[18] G. Royer, J. Phys. G, Nucl. Part. Phys. 26 (2000) 1149.
[19] V.Y. Denisov, H. Ikezoe, Phys. Rev. C 72 (2005) 064613.
[20] V.Y. Denisov, A.A. Khudenko, At. Data Nucl. Data Tables 95 (2009) 815.
[21] V.Yu. Denisov, O.I. Davydovskaya, I.Yu. Sedykh, Phys. Rev. C 92 (2015) 014602.
[22] B. Sahu, Phys. Rev. C 78 (2008) 044608.
[23] D.S. Delion, S. Peltonen, J. Suhonen, Phys. Rev. C 73 (2006) 014315.
[24] P. Roy Chowdhury, C. Samanta, D.N. Basu, Phys. Rev. C 73 (2006) 014612.
[25] Chang Xu, Zhongzhou Ren, Phys. Rev. C 73 (2006) 041301(R).
[26] M. Ismail, A. Adel, Phys. Rev. C 89 (2014) 034617;
M. Ismail, A. Adel, Phys. Rev. C 90 (2014) 064624.
[27] W.M. Seif, M. Shalaby, M.F. Alrakshy, Phys. Rev. C 84 (2011) 064608.
[28] W.M. Seif, J. Phys. G, Nucl. Part. Phys. 40 (2013) 105102.
[29] K.P. Santhosh, B. Priyanka, Phys. Rev. C 89 (2014) 064604.
[30] Dongdong Ni, Zhongzhou Ren, Nucl. Phys. A 828 (2009) 348.
[31] Yibin Qian, Zhongzhou Ren, Phys. Rev. C 88 (2013) 044329.
[32] Dongdong Ni, Zhongzhou Ren, Tiekuang Dong, Yibin Qian, Phys. Rev. C 87 (2013) 024310.
[33] Yibin Qian, Zhongzhou Ren, Dongdong Ni, Phys. Rev. C 89 (2014) 024318.
[34] F. Buchinger, J.M. Pearson, Phys. Rev. C 72 (2005) 057305.
[35] P. Möller, J.R. Nix, W.D. Myers, W.J. Swiatecki, At. Data Nucl. Data Tables 59 (1995) 185.
[36] Zaijun Wang, Zhongzhou Ren, Tiekuang Dong, Xiaoyong Guo, Phys. Rev. C 92 (2015) 014309.
[37] M. Warda, X. Viñas, X. Roca-Maza, M. Centelles, Phys. Rev. C 81 (2010) 054309.
[38] Jian Liu, Zhongzhou Ren, Chang Xu, Renli Xu, Phys. Rev. C 88 (2013) 024324.
[39] S. Abrahamyan, et al., PREX Collaboration, Phys. Rev. Lett. 108 (2012) 112502.
[40] C.M. Tarbert, et al., Crystal Ball at MAMI Collaboration, A2 Collaboration, Phys. Rev. Lett. 112 (2014) 242502.
[41] K. Wildermuth, Y.C. Tang, A Unified Theory of the Nucleus, Academic Press, New York, 1977.
[42] P.E. Hodgson, E. Běták, Phys. Rep. 374 (2003) 1.
[43] J.D. Walecka, Theoretical Nuclear and Subnuclear Physics, Oxford University, Oxford, 1995, p. 11.
[44] Yibin Qian, Zhongzhou Ren, Phys. Lett. B 738 (2014) 87.
[45] NNDC of the Brookhaven National Laboratory, http://www.nndc.bnl.gov.